

CONTENTS — N through Q

What is the Young's Modulus of Ice? <i>F. Nimmo</i>	7005
Lateral and Vertical Motions in Europa's Ice Shell <i>F. Nimmo</i>	7004
Domes on Europa: The Role of Thermally Induced Compositional Diapirism <i>R. T. Pappalardo and A. C. Barr</i>	7047
Numerical Modeling of Plate Motion: Unraveling Europa's Tectonic History <i>G. W. Patterson and J. W. Head III</i>	7038
Radar Sounding Studies for Quantifying Reflection and Scattering at Terrestrial Air-Ice and Ice-Ocean Interfaces Relevant to Europa's Icy Shell <i>M. E. Peters, D. D. Blankenship, and D. L. Morse</i>	7034
Impact Gardening, Sputtering, Mixing, and Surface-Subsurface Exchange on Europa <i>C. B. Phillips and C. F. Chyba</i>	7036
Clathrate Hydrates in Jupiter's Satellite Europa and Their Geological Effects <i>O. Prieto-Ballesteros, J. S. Kargel, M. Fernández-Sampedro, and D. L. Hogenboom</i>	7010
Geological Features and Resurfacing History of Europa <i>L. M. Prockter and P. H. Figueredo</i>	7056
European Bands Formed by Stretching the Icy Crust: A Numerical Perspective <i>R. Qin, W. R. Buck, and R. T. Pappalardo</i>	7030

WHAT IS THE YOUNG'S MODULUS OF ICE?. F. Nimmo, *Dept. Earth and Space Sciences, University of California Los Angeles, (nimmo@ess.ucla.edu).*

The Young's modulus E of ice is an important parameter in models of tidal deformation [1, e.g.] and in converting flexural rigidities to ice shell thicknesses [2, e.g.]. There is a disagreement of an order of magnitude between measurements of E in the laboratory (9 GPa) and from field observations (≈ 1 GPa). Here I use a simple yielding model to address this discrepancy, and conclude that $E = 9$ GPa is consistent with the field observations. I also show that flexurally-derived shell thicknesses for icy satellites are insensitive to uncertainties in E .

Lab Measurements Because ice may creep or fracture under an applied stress, it behaves elastically only if the loading frequency is high and stresses are small. Lower temperatures expand the parameter space in which elastic behaviour is expected. The most reliable way of determining E in the laboratory is to measure the sound velocity in ice and thus derive the elastic constants. The values of E found are consistently about 9 GPa [3; 4].

Field Measurements Field techniques rely on observing the response of ice shelves to tidal deformation [5]. In this case, loading frequencies are much lower ($\sim 10^{-5}$ Hz) and stresses much higher (~ 1 MPa). Fractures are commonly observed, and creep is also likely to occur [6]; thus, not all of the shelf may respond in an elastic fashion.

The length-scale of the response of an ice shelf to tidal deformation is determined by the parameter β [7], where:

$$\beta^4 = \frac{3\rho g (1 - \nu^2)}{ET_e^3}. \quad (1)$$

Here ρ is the density of the sea, g is the acceleration due to gravity, ν is Poisson's ratio and T_e is the effective elastic thickness of the ice shelf. The effective elastic thickness is defined as the thickness of a purely elastic plate which would produce the same response to loading as the actual ice shelf. Note that T_e will be less than the total ice shelf thickness h if ductile creep or fracture are important [8].

Field measurements of ice shelf deformation allow β to be determined [7]. Inspection of equation 1 shows that in order to derive E , a value for T_e must be assumed. One approach is to assume that the elastic thickness T_e is the same as the total ice shelf thickness h , which may be measured directly. Doing so results in values for E which are significantly smaller than the lab values. For instance, Vaughan [7] concluded that the effective Young's modulus from a variety of tidal deformation studies was 0.88 ± 0.35 GPa. [9] used radar observations of tidal flexure to conclude that E varied in both time and space, from 0.8 to 3.5 GPa. They ascribed the variation to viscoplastic effects. Similarly, [10] observed a time-delay between tidal forcing and ice-shelf response, which is also probably due to viscous effects.

Tension fractures are inferred to form at both the top and bottom of ice shelves due to tidal flexure, and may be tens of metres deep [11, p. 204]. The presence of these fractures will reduce the effective elastic thickness T_e of the ice shelf.

Furthermore, for typical curvatures of $10^{-6} m^{-1}$ and shelf thicknesses of 1 km (see Table 1), the maximum elastic stresses will be $O(1)$ MPa. These stresses are comparable to or exceed the likely elastic limit of ice [12] and suggest that much of the ice shelf will deform in a ductile rather than elastic fashion (see also [9]). It would therefore be surprising if the simple assumption that $T_e = h$ were correct. An alternative [5; 13] is to assume that the *effective* elastic thickness of the ice shelf is some fraction of the total shelf thickness. Doing so results in a larger value of E ; equation 1 shows that reducing T_e to 50% of the ice shelf thickness results in an eight-fold increase in E . This increase is sufficient to bring the field results into agreement with the laboratory measurements.

Yielding Model Below I develop a simple model to show the effect of ice yielding on T_e . It will be assumed that the ice is an elastic-perfectly plastic material [14] where the stress increases linearly with strain up to a particular yield stress, σ_y , and remains constant thereafter. The perfectly plastic regime represents the area in which either fracturing or ductile flow occurs.

The first moment of the stress-depth relationship for this rheology may be used to infer the effective elastic thickness T_e of the material [8]. Assuming that stress profile is symmetrical, it can be shown that

$$Te^3 = \frac{\sigma_y(1 - \nu^2)}{EK} \left(3h^2 - 4 \left[\frac{\sigma_y(1 - \nu^2)}{EK} \right]^2 \right) \quad (2)$$

where K is the curvature and it is assumed that $2\sigma_y(1 - \nu^2) < EK h$. If this inequality is not satisfied, the whole shelf behaves elastically and $T_e = h$.

The yield stress of ice is not well known, and probably varies with both temperature and strain rate. [12] argues that a yield stress of 0.1 MPa is appropriate for glacier ice. [15] show that the yield stress is independent of pressure, but depends on temperature and strain rate. Extrapolating their results to a strain rate of $10^{-8} s^{-1}$ suggests yield stresses of 0.6 MPa at $-5^\circ C$. A fracture depth of 10-100 m implies an effective yield stress of 0.1-1 MPa. I assume that $\nu=0.3$, $\rho = 1000 kg m^{-3}$, $g = 9.8 m s^{-2}$ and generally use $E=9$ GPa.

Table 1 lists the observational data from [7]. Rather than assuming that $T_e = h$, column 4 lists the implied value of T_e/h assuming that $E=9$ GPa and using equation 1. Column 5 lists the value of T_e/h obtained using the yielding model (equation 2). The agreement is generally quite good (except for Jakobshavn) and shows that yielding is a valid way of explaining the observations, and is consistent with the laboratory-derived value of E (9 GPa).

In summary, the observed flexure at ice shelves can be reconciled with the laboratory-determined values of E , if some fraction of the shelf experiences yielding (either fracture or creep). Yielding is expected to occur based on the likely behaviour of ice, and a simple elastic-plastic model shows that the amounts of yielding required are reasonable.

REFERENCES

location	$\beta \times 10^{-4}$ m^{-1}	h m	T_e/h (obs.)	T_e/h (theor.)
Rutford	2.4 ± 0.4	2000	0.48 ± 0.09	0.47
Ronne	$5.4 \pm_{1.5}^{2.7}$	700	$0.47 \pm_{0.27}^{0.15}$	0.46
Doake	3.4 ± 0.7	1000	0.61 ± 0.15	0.52
Bach	$11.0 \pm_{1.7}^{2.5}$	200?	$0.63 \pm_{0.16}^{0.11}$	0.54
Ekstrom	11.0 ± 0.7	150-200	0.72 ± 0.05	0.51-0.46
Jakobs- havn	$17.0 \pm_{2.0}^{4.0}$	450-800	$0.16 \pm_{0.04}^{0.02}$	0.47-0.38

Table 1: The values of β and h are obtained from [7]. T_e/h (obs.) is the value inferred from equation 1 using the observed β and h and assuming that $E=9$ GPa. T_e/h (theor.) is the value inferred from equation 2 assuming $\sigma_y=0.3$ MPa.

Icy satellites The ice shells of outer solar system satellites differ in several respects from terrestrial ice shelves. Firstly, strain rates are lower: around $10^{-10} s^{-1}$ on Europa, and less elsewhere. Secondly, surface temperatures are very much lower (typically 100-120 K), indicating that the ice may deform in a brittle fashion. Thirdly, the ice shells are probably 10's-100's km thick, implying that creep, rather than fracture, will occur towards the base of the ice shell. It is therefore more appropriate to use the yield-strength envelope (YSE) approach of [16; 8]. In this model, the near-surface ice deforms in a brittle manner, that at the base deforms in a ductile fashion, and that near the mid-plane elastically. The YSE approach allows us to convert a measurement of rigidity into a shell thickness, given a value for E . The conversion depends on the strain rate and curvature of the feature.

As an example, we will use an apparently flexural feature on Europa studied by [2]. We assume a conductive ice shell in which the thermal conductivity varies as $567/T$ and the top and bottom temperatures are 105 K and 260 K, respectively. The values of ρ, g and the coefficient of friction are $900 kg m^{-3}$, $1.3 m s^{-2}$ and 0.6, respectively. We will use the grain-boundary sliding ($n=2.4$) rheology of [17] which is grain-size independent. The strain rate is assumed to be $10^{-15} s^{-1}$.

[2] obtained a flexural parameter β of $6.25 \times 10^{-5} m^{-1}$ and a maximum curvature of $7.5 \times 10^{-7} m^{-1}$. Assuming a Young's modulus of 9 GPa, equation 1 gives $T_e=2.8$ km and the YSE approach gives a conductive ice shell thickness of 11 km. Taking $E=1$ GPa yields a T_e of 6 km and a shell thickness of 12 km. Increasing strain rate by two orders of magnitude decreases the inferred shell thickness by 1 km. Reducing the friction coefficient by 30% increases the shell thickness by 1 km. Using the grain-boundary sliding ($n = 1.8$) rheology of [17] with a grain-size of 1 mm reduces the shell thickness by 1 km. Thus, uncertainties in most parameters do not significantly affect the final result.

The shell thickness is insensitive to variations in E because the elastic portion of the shell is small. Hence, the YSE approach is a robust way of converting estimates of rigidity into ice shell thicknesses.

References

- [1] W. B. Moore and G. Schubert. The tidal response of Europa. *Icarus*, 147:317–319, 2000.
- [2] F. Nimmo, B. Giese, and R. T. Pappalardo. Estimates of Europa's ice shell thickness from elastically supported topography. *Geophys. Res. Lett.*, 30:1233, doi:10.1029/2002GL016660, 2003.
- [3] V. F. Petrenko and R. W. Whitworth. *Physics of Ice*. Oxford Univ. Press, New York, 1999.
- [4] P. H. Gammon, H. Kiefte, M. J. Clouter, and W. W. Denner. Elastic constants of artificial and natural ice samples by Brillouin spectroscopy. *J. Glaciol.*, 29(103):433–460, 1983.
- [5] G. Holdsworth. Tidal interaction with ice shelves. *Ann. Geophys.*, 33(1):133–146, 1977.
- [6] T. J. Hughes. West Antarctic ice streams. *Rev. Geophys. Space Phys.*, 15(1):1–46, 1977.
- [7] D. G. Vaughan. Tidal flexure at ice shell margins. *J. Geophys. Res.-Solid Earth*, 100(B4):6213–6224, 1995.
- [8] A. B. Watts. *Isostasy and flexure of the lithosphere*. Cambridge Univ. Press, Cambridge, 2001.
- [9] M. Schmeltz, E. Rignot, and D. MacAyeal. Tidal flexure along ice-sheet margins: comparison of insar with an elastic-plate model. *Annals Glaciology*, 34:202–208, 2002.
- [10] N. Reeh, C. Mayer, O. B. Olesen, E. L. Christensen, and H. H. Thomsen. Tidal movement of Nioghalvfjordsfjorden glacier, northeast Greenland: observations and modelling. *Ann. Glaciol.*, 31:111–117, 2000.
- [11] T. Hughes. *Ice Sheets*. Oxford Univ. Press, New York, 1998.
- [12] W. S. B. Paterson. *The Physics of Glaciers*. Pergamon Press, New York, 1981.
- [13] C. S. Lingle, T. J. Hughes, and R. C. Kollmeyer. Tidal flexure of Jakobshavns glacier, West Greenland. *J. Geophys. Res.*, 86(B5):3960–3968, 1981.
- [14] D. L. Turcotte and G. Schubert. *Geodynamics*. John Wiley and Sons, New York, 1982.
- [15] M. A. Rist and S. A. F. Murrell. Ice triaxial deformation and fracture. *J. Glaciol.*, 40(135):305–318, 1994.
- [16] M. K. McNutt. Lithospheric flexure and thermal anomalies. *J. Geophys. Res.*, 89(NB13):11180–11194, 1984.
- [17] D. L. Goldsby and D. L. Kohlstedt. Superplastic deformation of ice: Experimental observations. *J. Geophys. Res.-Solid Earth*, 106(B6):11017–11030, 2001.

LATERAL AND VERTICAL MOTIONS IN EUROPA'S ICE SHELL. F. Nimmo, *Dept. Earth and Space Sciences, University of California Los Angeles, (nimmo@ess.ucla.edu).*

Characterizing the lateral and vertical motions that occur within Europa's ice shell is challenging but important. Vertical motions can transport nutrients and thus have astrobiological importance, while lateral movements can cause thinning of the ice shell. Future mission design will be affected by what we think we know about the characteristics of Europa's ice shell. Models and inferences of vertical and lateral motion will help us to constrain the ice shell thickness, and also to estimate the characteristic strain rates and stresses (ie. the shell dynamics).

LATERAL MOTION

Lateral extension is very obvious in bands [1], though minor amounts of strike-slip or compressive motion may also occur [2; 3]. The localized, high stretching factor rifting is very different to the diffuse, lower stretching factor extension seen on Ganymede. Localized extension is favoured by high strain rates and low shell thicknesses. Recent work by [4] suggests that an extensional strain rate $> 10^{-15} \text{ s}^{-1}$ is required to form bands on Europa. The associated stresses are $\approx 0.3 \text{ MPa}$, similar to estimates inferred from flexural studies but several orders of magnitude larger than present day tidal stresses. The fact that bands appear to be elevated relative to their surroundings suggests either compositional or (recent) thermal buoyancy [5].

A less obvious but equally important kind of lateral motion is flow in the lowermost part of the shell. Lateral shell thickness contrasts, *even if isostatically compensated*, produce pressure gradients which drive flow. Thus, topography produced by lateral shell thickness contrasts decays with time [6]. The rate of decay can be very rapid, especially for thick shells. However, the rate of decay is slower for non-Newtonian materials, such as ice, than it is for Newtonian ones. Global shell thickness contrasts can probably be maintained for 50 Myr, but local ($\sim 100 \text{ km}$) variations cannot [7].

Strike slip motion has also been identified on Europa [3] and is almost certainly driven by a "tidal walking" process [8]. It has been proposed that shear-heating at such sites could lead to the formation of double ridges [9]. If shear heating leads to melting, this provides a potential source of near-surface liquid water. Finally, shear heating zones are a source of weakness, which may explain why many bands appear to initiate at double ridges.

Compressional motion is rare on Europa, though folds have been identified in one area [10]. The imbalance between extension and compression is a puzzle. It is possible that compression is being accommodated by diffuse shortening which leaves little geological evidence.

VERTICAL MOTION

The evidence for vertical motion is less clear than that for lateral movements. Features termed pits, spots and domes may be the surface expression of subsurface vertical motion [11], but there is a lack of agreement on this point [12]. Even more controversially, chaos terrains may be the result of either diapiric activity [13] or melt-through caused by hydrothermal

plumes [14]. A second kind of vertical motion occurs due to surface, rather than subsurface loads.

Thermal convection suffers from two problems in explaining the surface features. Firstly, it is much harder to initiate convection in Newtonian than non-Newtonian materials [15]. Furthermore, for the likely grain sizes and strain rates, the deformation of ice is controlled by the *slower* of the two relevant mechanisms [16]. The overall result is that convection is unlikely to occur unless the shell thickness exceeds 50 km This is substantially larger than earlier estimates of the critical shell thickness [11; 17].

Secondly, the temperature contrast generated by strongly temperature-dependent convection is determined by the rheological properties of the ice, and is small ($\sim 10 \text{ K}$) [15]. This temperature contrast is probably too small to generate the observed dome amplitudes of several hundred metres [18; 19]. Although a tidal feedback mechanism has been proposed [20], it is not clear that the very long wavelength tidal deformation will couple efficiently with the much shorter wavelength diapiric features [W. Moore, pers. comm.].

Compositional convection is an alternative mechanism for diapir formation. [5] proposed that compositional density contrasts might arise through the preferential loss of brines from warm ice. In this scenario, warm ice near the base of the shell loses salts, is more buoyant than the colder ice overlying it, and becomes gravitationally unstable. This Rayleigh-Taylor instability will grow most rapidly at a characteristic wavelength, which will determine the size of the ascending diapirs [21]. For most systems, the characteristic wavelength is a few times the thickness of the layer above the instability. The rise time of the resulting diapir depends on its radius r , density contrast $\Delta\rho$ and the viscosity structure of the ice. For viscosity which increases exponentially upwards with a characteristic length-scale δ , the rise time τ is given by

$$\tau \approx \frac{\eta_0 \delta}{r^2 \Delta\rho g} (\exp(h/\delta) - 1) \quad (1)$$

where g is gravity, η_0 is the viscosity at the base of the shell and h is the shell thickness. For likely diapir radii ($\sim 5 \text{ km}$) and ice viscosities ($\sim 10^{14} \text{ Pa s}$), the rise time is $O(1 \text{ Myr})$. The nature of the return flow mechanism in the case of compositional convection is not clear, but may involve broad-scale downwards motion.

Vertical motions in response to surface loading also occur. The horizontal distance over which the deformation occurs provides information about the elastic thickness of the ice shell [22; 23]. Frequently, the margins of chaos terrain are a few hundred metres lower than the surrounding areas, and appear to have downdropped along sharp contacts [22]. This downdropping is consistent with scenarios in which the underlying ice is thinned (or even completely melted). While chaos terrain may be elevated with respect to the surroundings at the present day [13], this topography may post-date the original formation of the chaos.

REFERENCES

Summary and Future Questions

The availability of topographic data is now allowing us to place quantitative constraints on processes happening within Europa's ice shell. However, as yet neither the *spatial* nor the *temporal* variations in these processes have been properly addressed. Temporal variations are detectable with geological mapping; spatial variations are dependent on data availability. It is therefore critically important to maximize the amount of data available, which in practice will mean increasing reliance on photoclinometric methods [24].

The estimation of stresses and strain rates within Europa's ice shell is at an early stage. However, it is already clear that many of the features observed imply stresses far in excess of the present-day tidal stresses. Other sources of stress, such as those due to compositional or thermal buoyancy, must also be present. Again, whether there are temporal or spatial variations in stress or strain will be the subject of future investigations. Similarly, the reconciliation of global models of tidal dissipation with local geological features has barely begun.

References

- [1] L. M. Prockter, J. W. Head, R. T. Pappalardo, R. J. Sullivan, A. E. Clifton, B. Giese, R. Wagner, and G. Neukum. Morphology of European bands at high resolution: A mid-ocean ridge-type rift mechanism. *J. Geophys. Res.-Planets*, 107(E5):5028, doi:10.1029/2000JE001458, 2002.
- [2] B. R. Tufts, R. Greenberg, G. Hoppa, and P. Geissler. Lithospheric dilation on Europa. *Icarus*, 146(1):75–97, 2000.
- [3] A. R. Sarid, R. Greenberg, G. V. Hoppa, T. A. Hurford, B. R. Tufts, and P. Geissler. Polar wander and surface convergence of Europa's ice shell: evidence from a survey of strike-slip displacement. *Icarus*, 158:24–41, 2002.
- [4] F. Nimmo. Dynamics of rifting and modes of extension on icy satellites. *J. Geophys. Res. -Planets*, page in press, 2003.
- [5] F. Nimmo, R. T. Pappalardo, and B. Giese. On the origins of band topography, Europa. *Icarus*, 166:21–32, 2003.
- [6] D. J. Stevenson. Limits on the variation of thickness of Europa's ice shell. *Lun. and Planet. Sci. Conf.*, XXXI:art. no. 1506, 2000.
- [7] F. Nimmo. Non-Newtonian topographic relaxation on Europa. *Icarus*, page submitted, 2003.
- [8] G. V. Hoppa, B. R. Tufts, R. Greenberg, and P. E. Geissler. Strike-slip faults on Europa: global shear patterns driven by tidal stress. *Icarus*, 141:287–298, 1999.
- [9] F. Nimmo and E. Gaidos. Strike-slip motion and double ridge formation on Europa. *J. Geophys. Res.-Planets*, 107(E4):5021, doi:10.1029/2000JE001476, 2002.
- [10] L. M. Prockter and R. T. Pappalardo. Folds on Europa: implications for crustal cycling and accommodation of extension. *Science*, 289(5481):941–943, 2000.
- [11] R. T. Pappalardo and et. al. Geological evidence for solid-state convection in Europa's ice shell. *Nature*, 391:365–368, 1998.
- [12] R. Greenberg, M. A. Leake, G. V. Hoppa, and B. R. Tufts. Pits and uplifts on Europa. *Icarus*, 161:102–126, 2003.
- [13] P. M. Schenk and R. T. Pappalardo. Stereo and photoclinometric topography of chaos and anarchy on Europa. *Lun. and Planet. Sci. Conf.*, XXXIII:art. no. 2035, 2002.
- [14] D. P. O'Brien, P. Geissler, and R. Greenberg. A melt-through model for chaos formation on Europa. *Icarus*, 156(1):152–161, 2002.
- [15] F. Nimmo and M. Manga. Causes, characteristics and consequences of convective diapirism on Europa. *Geophys. Res. Lett.*, 29(23):2109, doi:10.1029/2002GL015754, 2002.
- [16] D. L. Goldsby and D. L. Kohlstedt. Superplastic deformation of ice: Experimental observations. *J. Geophys. Res.-Solid Earth*, 106(B6):11017–11030, 2001.
- [17] W. B. McKinnon. Convective instability in Europa's floating ice shell. *Geophys. Res. Lett.*, 26(7):951–954, 1999.
- [18] A. P. Showman and L. Han. Numerical simulations of convection in Europa's ice shell: implications for surface features. *Lun. and Planet. Sci. Conf.*, XXXIV:art. no. 1806, 2003.
- [19] A.C. Barr and R.T. Pappalardo. Numerical simulations of non-newtonian convection in ice: application to Europa. *Lun. and Planet. Sci. Conf.*, XXXIV:art. no. 1477, 2003.
- [20] C. Sotin, J. W. Head, and G. Tobie. Europa: Tidal heating of upwelling thermal plumes and the origin of lenticulae and chaos melting. *Geophys. Res. Lett.*, 29(8):art. no. 1233, 2002.
- [21] D. L. Turcotte and G. Schubert. *Geodynamics*. John Wiley and Sons, New York, 1982.
- [22] P. Figueredo, R. L. Kirk F. C. Chuang, J. Rathbun, and R. Greeley. Geology and origin of Europa's Mitten feature (Murias Chaos). *J. Geophys. Res.*, 107(E5):5026, doi:10.1029/2001JE001591, 2002.
- [23] F. Nimmo, B. Giese, and R. T. Pappalardo. Estimates of Europa's ice shell thickness from elastically supported topography. *Geophys. Res. Lett.*, 30:1233, doi:10.1029/2002GL016660, 2003.
- [24] R.L. Kirk, J. M. Barrett, and L. A. Soderblom. Photoclinometry made simple . . . ? *Advances in Planetary Mapping*, Houston, 2003.

DOMES ON EUROPA: THE ROLE OF THERMALLY INDUCED COMPOSITIONAL DIAPIRISM. R. T. Pappalardo and A. C. Barr, University of Colorado, Boulder, CO 80309-0397 (robert.pappalardo@colorado.edu).

Overview: The surface of Europa is peppered by topographic domes, interpreted as sites of intrusion and extrusion. Diapirism is consistent with dome morphology, but thermal buoyancy alone cannot produce sufficient driving pressures to create the observed dome elevations. Instead, we suggest that diapirs may initiate by thermal convection that induces compositional segregation within Europa's ice shell. This double-diffusive convection scenario allows sufficient buoyancy for icy plumes to create the observed surface topography, if the ice shell has a very small effective elastic thickness (~ 0.1 to 0.5 km) and contains low-eutectic-point impurities at the percent level.

Thermal Buoyancy: Thermal diapirism has been proposed as a source of buoyancy for forming Europa's domes [1,2]. Solid-state convection is capable of bringing warm material to shallow (several km) depths within Europa's ice shell [3]; however, stresses due to thermally driven convection are small. The maximum convective stress is

$$P_d \sim 0.1 \rho_i g \alpha T D \quad (1)$$

[4], where ρ_i is ice density, g is gravitational acceleration (1.3 m s^{-2} for Europa), α is the coefficient of thermal expansion, T is the temperature difference across the ice shell, and D is the ice shell thickness.

For $\alpha = 10^{-4} \text{ K}^{-1}$ and $T = 160 \text{ K}$, the $P_d \sim 4 \times 10^4$ Pa within an ice shell of $D \approx 20$ km thickness. Numerical modeling of convection and associated thermal diapirism supports this analysis, predicting relief of only ~ 10 m above convective upwellings [5].

Diffusive cooling can cause diapirs to stall in the subsurface [2]. If warm diapirs reach the surface, thermal diffusion further robs buoyancy, and domes relax as they cool [6] if not supported by dynamic processes or compositional density variations [cf. 7].

Compositional Buoyancy and Double-Diffusive Convection: Differences in impurity levels serve as a potential source of compositional buoyancy to drive diapiric rise, and may be relevant to Europa dome formation (Fig. 1). Galileo NIMS results indicate non-ice materials on Europa, modeled as hydrated sulfate salts [8] or sulfuric acid hydrate [9], but the level of contaminants within the ice is highly uncertain.

A convecting icy shell is expected to have a nearly isothermal adiabatic temperature, T_{ad} , beneath a rigid stagnant lid. For a basally heated pure ice shell, T_{ad} can be as low as $\sim 245 \text{ K}$ [3], while for an internally (tidally) heated ice shell, T_{ad} is 250 to 260 K [6,10].

Both sulfate and chloride contaminants are plausible constituents of Europa's icy shell [11]. Hydrated sulfate salts have eutectic temperatures [12] $\sim 270 \text{ K}$, securely above the predicted T_{ad} for Europa; therefore, these salts are expected to be stable against eutectic melting. However, the eutectic temperatures of hydrated chloride salts are in the range ~ 220 to 250 K ,

i.e. less than or comparable to the expected T_{ad} . Moreover, the ice- H_2SO_4 system has a eutectic of 211 K [11]. If hydrated chloride salts or sulfuric acid (herein collectively termed "low-eutectic" contaminants) exist within Europa's ice shell, they are expected to melt and produce brines in response to thermal convection. This should be the case throughout the warm base of the ice shell, and wherever a warm ice plume contacts colder contaminant-rich ice.

Melt is expected to drain through the ice at $\sim 10 \text{ m yr}^{-1}$ [13], significantly faster than the ~ 0.1 to 1 m yr^{-1} vertical velocity of convective ice plumes [3]. Therefore, the warm base of the ice shell and the convective plumes that rise from it are expected to be relatively clean of low-eutectic impurities (Fig. 1). In this model, low-eutectic contaminants are expected to become depleted in the ice shell over time unless replenished. It is plausible that Europa's ice shell is not in steady-state, but that instead its youthful surface age (~ 30 to 80 Myr [14]) reflects a latest incarnation of the ice shell, which began as relatively contaminant-rich and is more recently depleted in contaminants over time.

The warmer ice of a rising diapir will be cleaner and thus compositionally buoyant relative to its surroundings. Assuming isostasy above a column cleaned of low-eutectic contaminants through diapiric rise,

$$P_d = \rho (\rho_e - \rho_b) g D \quad (2)$$

where ρ_e is the average density of the low-eutectic solids, ρ_b is the ambient density of the impure ice shell, and ρ is the volume fraction of low-eutectic contaminants that melt and drain from diapiric plumes.

Choosing $\rho_b = 1000 \text{ kg m}^{-3}$ and $\rho_e = 1500 \text{ kg m}^{-3}$, $\rho \sim 2\%$ can produce $P_d \sim 10^5 \text{ Pa}$ for a range of reasonable ice shell thicknesses, sufficient to upwarp domes to observed ($\sim 100 \text{ m}$) heights for intrusions beneath a brittle ice cover of $T_e \sim 0.1$ to 0.5 km for Young's modulus $E \sim 10^9$ to 10^{10} Pa . The minor amounts of low-eutectic contaminants required are consistent with geochemical models of Europa's evolution [11].

The thermo-compositional buoyancy scenario envisioned here is essentially one of double-diffusive convection (DDC), in which both thermal and compositional gradients exist to trigger fluid motions [e.g., 15], as governed by the standard thermal Rayleigh number

$$\text{Ra} = \rho g \alpha T D^3 / \mu \kappa \quad (3)$$

(where α is the coefficient of thermal expansion, T is the temperature drop across the convecting layer, κ is the thermal diffusivity, and μ is viscosity), as well as a compositional Rayleigh number

$$\text{Ra}_c = \rho g \Delta C D^3 / \mu \kappa \quad (4)$$

(where ΔC is a compositional counterpart to T , and κC is the vertical composition gradient across the convecting layer).

The system operates in the "finger" regime, where compositionally buoyant material can rise in narrow

upwellings of scale much smaller than the thickness of the convecting system, if

$$Ra_c - Ra > \frac{27}{4} \Gamma^4 \quad (5)$$

[16], whereas the system is in the diffusive regime typical of thermal convection for lesser values of $(Ra_c - Ra)$. This relationship can also be expressed in terms of temperature and concentration gradients as

$$\frac{\rho_b g D^4}{\Gamma} \left[\frac{\Gamma C}{\rho_c D} - \frac{\Gamma T}{D} \right] > 657 \quad (6)$$

where Γ_c is the compositional diffusivity. For concentrations expressed as volume fraction f , then $\Gamma C = \Gamma f$, and $\Gamma = (\rho_e - \rho) / \rho$.

For Europa, the value of Γ_c can be envisioned as governed by the melt composition, the velocity of melt drainage v_m , and a characteristic length scale for melt drainage L , as

$$\Gamma_c \sim \Gamma_e \Gamma v_m L \quad (7)$$

where Γ_e is the volume fraction of low-eutectic contaminants in the melt. The length scale L is unknown but may be in the range ~ 1 to 10% of the scale of a diapir, or ~ 70 to 700 m. Choosing plausible values of $\Gamma \sim 0.02$, $\Gamma_e \sim 0.1$, and $v_m \sim 10 \text{ m yr}^{-1}$, then $\Gamma_c \sim 4 \times 10^7$ to $4 \times 10^8 \text{ m}^2 \text{ s}^{-1}$. Assuming a mean ice viscosity of $\sim 10^{18} \text{ Pa s}$, $\Gamma \sim 10^4 \text{ m}^2 \text{ s}^{-1}$, $\Gamma T \approx 160 \text{ K}$, and $D \sim 20 \text{ km}$, then $(Ra_c - Ra) \sim 250$ to 2500. This suggests that Europa's ice shell may be transitional between the diffusive and finger regimes, but uncertainty in L and Γ_c implies that this coarse estimate must be refined.

Summary and Implications: The required buoyancy to account for Europa's domes is difficult to achieve through thermal convection alone but can be produced by percentage level compositional differences between ice diapirs and their surroundings, if low-eutectic contaminants melt and drain from warm ice plumes, and if the effective thickness of the brittle lithosphere is very small (~ 0.1 to 0.5 km). This implies that convection in Europa's ice shell is best modeled as double-diffusive convection, in which thermal and compositional gradients are both important. Convection in the compositionally dominated finger regime can result in upwelling diapirs that are significantly smaller in scale than the vertical scale of the convecting medium, so attempts to relate lenticula size to Europa's ice shell thickness may not be fruitful.

Thermally induced compositional buoyancy offers a comprehensive and geophysically plausible means for forming Europa's domes. An analogous model has been applied to Europa's bands by [7], and is potentially applicable to the satellite's larger chaos regions as well. The model implies significant compositional inhomogeneity on a local scale within the ice shell, which might be directly detectable by future missions using ground penetrating radar. This process would allow deep interior material to breach the Europa's cold brittle lithosphere, with potential implications for transport of oceanic and astrobiologically relevant materials to the surface.

Acknowledgements: Supported is provided by NASA Exobiology grant NCC2-1340 and GSRP NGT5-50337.

References: [1] Pappalardo, R. T., et al., *Nature*, 391, 365-368, 1998. [2] Rathbun, J. A., et al., *Geophys. Res. Lett.*, 25, 4157-4160, 1998. [3] Barr, A. C. and R. T. Pappalardo, *LPSC XXXIV*, # 1477, 2003. [4] McKinnon, W. B., in *Solar System Ices*, pp. 525-550, 1998. [5] Showman, A. P. and L. Han, *LPSC XXXIV*, #1806, 2003. [6] Nimmo, F. and M. Manga, *GRL*, 29(23), 10.1029/2002GL015754, 2002. [7] Nimmo, F., et al., *Icarus*, 166, 21-32, 2003. [8] McCord, T. B., et al., *JGR*, 103, 8603-8626, 1998. [9] Carlson, R. W., et al., *Science*, 286, 97-99, 1999. [10] McKinnon, W. B., *GRL*, 26, 951-954, 1999. [11] Kargel, J. S., et al., *Icarus*, 148, 226-265, 2000. [12] Brass, G. W., *Icarus*, 42, 20-28, 1980. [13] Gaidos, E. and F. Nimmo, *Nature*, 405, 637, 2000. [14] Zahnle, K., et al., *Icarus*, 163, 263-289, 2003. [15] Hansen, U., and D. A. Yuen, *Earth Sci. Rev.*, 29, 385-399, 1990. [16] Kundu, P., *Fluid Mechanics*, Academic Press, 1990.

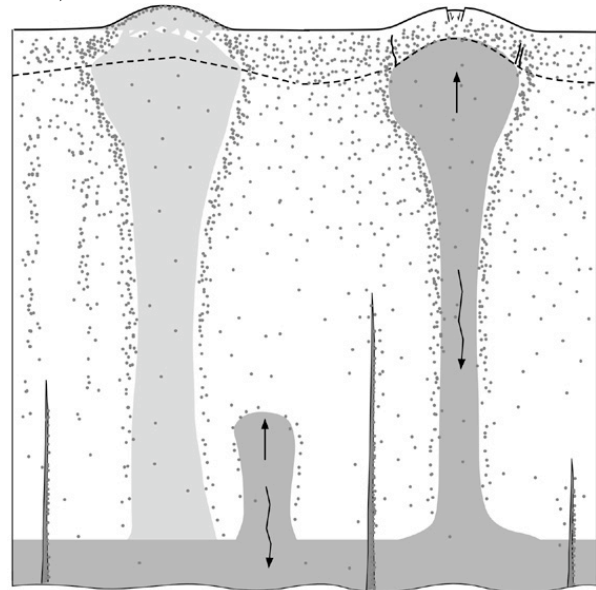


Fig. 1: Schematic illustration of the thermally induced compositional diapirism model. As warm ice (dark gray) near the base of Europa's ice shell begins to rise diapirically, it melts overlying low-eutectic contaminants (stipples) and the brines drain downward (squiggly arrows), allowing compositional buoyancy to aid diapir rise toward the surface. Buoyant diapiric material can breach the cold brittle lithosphere and extrude to form a dome (left); contaminants remaining in the diapiric ice are then concentrated by exogenic processes. Alternatively, diapirs can intrude and upwarp the brittle lithosphere to form intrusive domes (right). Low-eutectic contaminant concentration is least in the warmest ice and locally concentrated in halos surrounding diapirs from which they have been expelled. Dome topography and subsurface compositional gradients persist whether the underlying ice column is warm or has cooled (left, lighter gray), until subsequent diapirism redistributes the constituents. Diking might replenish some contaminants from the ocean below, but the ice shell is expected to be overall depleted in low-eutectic contaminants over time.

NUMERICAL MODELING OF PLATE MOTION: UNRAVELING EUROPA'S TECTONIC HISTORY.

G. W. Patterson and J. W. Head III, Department of Geological Sciences, Brown University, Providence, RI , 02912 (Gerald_Patterson@brown.edu).

Introduction: Europa is a highly fractured body broken into plates that have rotated with respect to one another. The effect of these rotations can be seen as regions of extension, strike-slip motion, and possibly compression [1,2,3,4]. Various authors have tried to reconstruct a number of these regions in an effort to gain a better understanding of the tectonic history of the icy satellite [4-8].

The typical approach used to determine a best-fit reconstruction could be described as a 'cut-and-paste' method in which the plates in an image are manually separated and reoriented in an effort to reconstruct preexisting features [4,5,6]. Some authors subsequently determined poles of rotation for the regions reconstructed [7,8]. This step is essential to determining the validity of a reconstruction when the size of a region is such that the curvature of the satellite cannot be ignored.

In those cases that have looked for a pole of rotation, a forward approach is typically used. This method can be used to show that the reconstruction produced has a unique solution but it cannot tell whether or not there were other unique solutions that were not considered. Here we report on the development of an inverse method for determining the Euler pole of a region that has undergone rotation. This method can be used to test all possible rotations of the region and therefore determine all unique solutions (if they exist).

The Model. The inverse model we have developed uses an iterative grid-search method to find an Euler pole of rotation for the region to be reconstructed such that ridges cut and offset will be re-aligned. The result is a minimized best-fit pole with confidence regions. This is a brute force method that is mathematically simple but computationally cumbersome. The computational requirements of this modeling technique limit the resolution of the grid that can be used to determine the Euler pole but it is sufficient to fully resolve the pole for the resolution of the image used.

$$\begin{aligned}
 N_x &= (A_y * B_z - A_z * B_y) / \sin \delta \\
 N_y &= (A_z * B_x - A_x * B_z) / \sin \delta \\
 N_z &= (A_x * B_y - A_y * B_x) / \sin \delta \\
 \delta &= \cos^{-1} (A_x * B_x + A_y * B_y + A_z * B_z)
 \end{aligned}
 \tag{1}$$

The model uses two points (A and B) on a fixed plate to form a plane through the body (Fig. 1). The normal to that plane is determined using equation 1 and the distance from that plane to a point (C) on the plate to be reconstructed that corresponds to the offset feature of the fixed plate is determined using equation 2.

$$dist = \left| \overline{AC}_x * N_x + \overline{AC}_y * N_y + \overline{AC}_z * N_z \right| \tag{2}$$

A best-fit reconstruction of the points described involves rotating point C on the plate to be reconstructed about an Euler pole such that it falls in the plane of points A and B on the fixed plate. To accomplish this we use a rotation matrix (equation 3), where R_{ij} is the rotation matrix and it is defined by an Euler pole $E = (E_x, E_y, E_z)$ and an angle of rotation Ω [9].

$$\begin{bmatrix} C_{x'} \\ C_{y'} \\ C_{z'} \end{bmatrix} = \begin{bmatrix} R_{11} & R_{12} & R_{13} \\ R_{21} & R_{22} & R_{23} \\ R_{31} & R_{32} & R_{33} \end{bmatrix} * \begin{bmatrix} C_x \\ C_y \\ C_z \end{bmatrix} \tag{3}$$

Confidence regions for the determined pole were calculated using the following equation [10]:

$$R = R_{\min} \left(1 + (N / M - N) F [N, M - N, 1 - \alpha] \right)^{1/2} \tag{4}$$

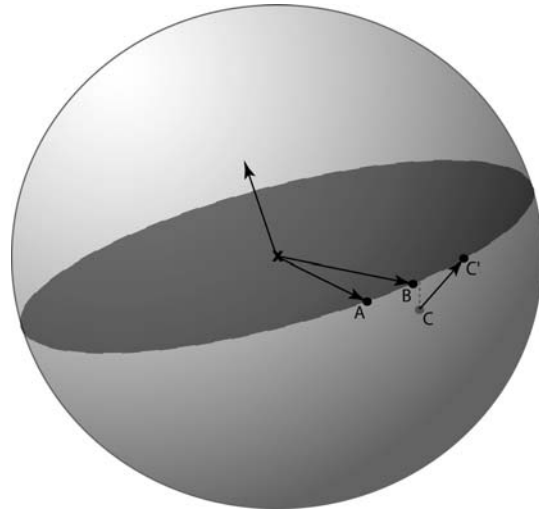


Fig. 1. Illustration of inverse modeling technique. A and B represent points on an offset feature lying on a fixed plate and C represents a point on the same offset

feature lying on the plate to be rotated. C' represents the position of the offset feature after rotation.

A Test Case: The Castalia Macula region was chosen as a test case for the application of this inverse method (Fig. 2). The region in the image is centered about the equator and spans ~ 800 km. We rotated one plate in this region that is marked by numerous offset features, 27 of which were used in this analysis (the main criterion for choosing these features was clarity of the precise location of each feature across the plate boundary).

The model determined the Euler pole that minimized the distance between the offset features after iterating through every possible combination of pole location and rotation. The resolution of the grid used was increased steadily until we reached the resolution limit of the image. Figure 3 indicates the location of the best-fit pole for this region. The final grid employed was a $1^\circ \times 1^\circ$ latitude/longitude grid with possible rotations tested ranging from -1° to 1° in $.01^\circ$ increments. The pole location is 11° lat. and 253° lon. with -0.43° rotation and the post reconstruction misfit of previously offset features for this reconstruction is within the resolution of the image. This, along with the tightly constrained confidence regions, indicates that a best-fit Euler pole for the region in question has been determined.

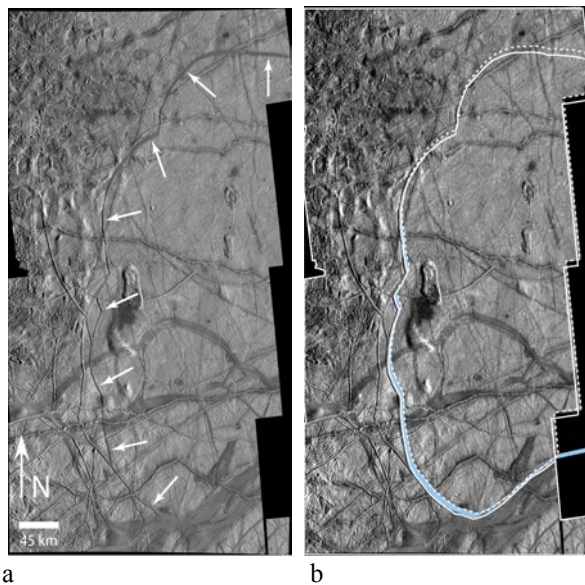


Fig. 2. Castalia Macula region (centered at $\sim 0^\circ$ lat and 227° lon) as seen in Galileo E17REGMAP01 mosaic (a). Image is transmercator projected with resolution of $220\text{m}/\text{pix}$. Arrows indicate ridge that was reconstructed. Reconstruction of region (b) using Euler pole and rotation shown in Fig. 3. Solid line indicates position of plate before reconstruction and dashed line indicates position after.

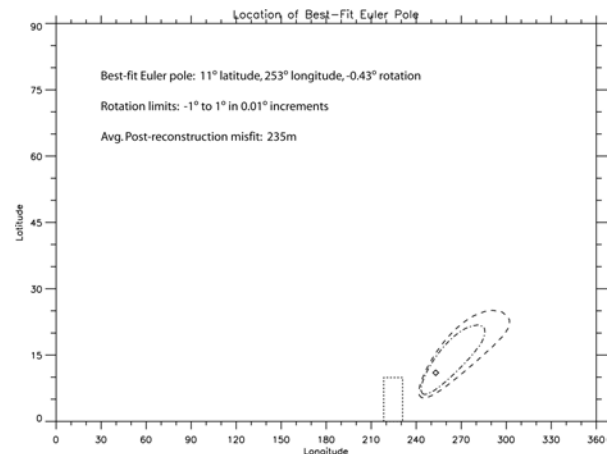


Fig. 2. Plot indicating position of best-fit Euler pole for Castalia Macula region. Dashed lines represent 95% and 99% confidence regions.

Conclusions and Implications: The test case for this method demonstrates that a unique solution for the Euler pole of rotation of this region can be determined. Knowledge of this unique solution allows us to produce a reconstruction of the plate motion in this region with an accuracy that can be quantified. Application of this method to other regions could provide a powerful means of unraveling the tectonic history of Europa.

The application of this model is presently limited by the spatial resolution and coverage available from the Voyager and Galileo missions. Increased image resolution and global comprehensive coverage by future missions will allow us to constrain pole locations and degree of rotation with increased accuracy as well as to consider the broader implications of regional plate rotations on Europa's global tectonic history.

Acknowledgements: We would like to thank Donald Forsyth for his assistance in developing the inverse model.

References: [1] Greeley et al., *Icarus*, 135, 4-24, 1998. [2] Hoppa et al., *Icarus*, 141, 287-298, 1999. [3] Prockter, L.M., and R. T. Pappalardo, *Science*, 289, 941-943, 2000. [4] Patterson, G.W. and R.T. Pappalardo, *Lunar Planet. Sci. Conf. XXXIII*, abstract # 1681 [5] Tufts et al., *Icarus*, 146, 57-75, 2000. [6] Sarid et al., *Icarus*, 158, 24-41, 2002. [7] Schenk, P.M., and W.B. McKinnon, *Icarus*, 79, 75-100, 1989. [8] Pappalardo, R. T. and R. J. Sullivan, *Icarus*, 123, 557-567, 1996. [9] Cox and Hart (1986), *Plate tectonics*, Blackwell Scientific Publications, 51-84 [10] Draper and Smith, *Applied Regression Analysis*, John Wiley and Sons Inc., 1996.

RADAR SOUNDING STUDIES FOR QUANTIFYING REFLECTION AND SCATTERING AT TERRESTRIAL AIR-ICE AND ICE-OCEAN INTERFACES RELEVANT TO EUROPA'S ICY SHELL.

M. E. Peters¹, D. D. Blankenship¹ and D. L. Morse¹, ¹University of Texas, Institute for Geophysics, 4412 Spicewood Springs Rd, Bldg 600, Austin, TX, 78759 (mattp@ig.utexas.edu).

Introduction: Jupiter's moon Europa is characterized by a pervasive icy mantle underlain by a global ocean. The distribution of free water and brines within Europa's icy/watery shell and the processes within the ice that control the exchange of material both with the surface and the ocean will determine Europa's suitability for harboring life. On Earth's ice sheets, radar sounding has proven to be a powerful tool for characterizing the ice-ocean interface as well as the overlying ice up to and including the air-ice interface. We present radar sounding techniques and new results from our recent airborne radar studies over ice-ocean environments in Antarctica.

Geologic Background: Certain processes hypothesized to occur for Europa's icy mantle and ocean have terrestrial analogs in the grounding zones of Antarctic ice streams [1-4]. These dynamic systems involve the interaction of the moving ice mass with the underlying materials, including liquid water (see Figure 1). Surface crevasses at varying levels accompany the ice streams due to high shear stresses at the ice stream margins. Bottom crevasses generally result at the grounding line due to tidal flexure. Once afloat, the ice and its interfaces continue to evolve. Ablation and accretion processes affect the character of the ice-ocean interface. Old bottom crevasses are healed, while new ones can be created, sometimes extending through the full ice thickness (see Figure 2). These processes continue beyond the calving of icebergs at the ice shelf front.

Imaging and characterizing the subglacial environment is fundamental to understanding these complex systems. Our focus has been to characterize the basal interface over the grounding zone of ice stream C and the ice-ocean interface of iceberg B-15 through radar reflection and scattering analyses. We also apply these techniques to the air-ice interface.

Echo Theory and Radar Methods: Echoes from the basal interface generally consist of both specularly reflected and diffusely scattered energy. Subglacial echoes are influenced by physical properties of the interface such as the composition, uniformity and roughness of the materials at the interface. Other important factors include dielectric losses and volumetric scattering losses from propagation through the ice as well as transmission at the air-ice interface. The primary physical factors influencing echoes from the air-ice interface are the surface roughness, the presence of surface crevasses, and the density of the air-ice mixture (firn).

Radar sounding techniques are well-suited to characterizing the reflection and scattering nature of both the ice-ocean and air-ice interfaces [5,6]. For example, unfocussed synthetic aperture radar (SAR) narrows the along-track radar beam, thus increasing resolution and the likelihood of specular reflection from the subglacial interface. Also, echo amplitude statistics can be used to identify reflecting or scattering regions. Fading analyses utilizing both echo

ing regions. Fading analyses utilizing both echo amplitude and phase can provide estimates of the off-nadir extent of returned echoes, relating to scattering from the interface.

Radar System: Our radar system uses a programmable signal source with a dual-channel coherent down-conversion receiver [7] linked to a 10 kW transmitter. The radar operates in chirped pulse mode at 60 MHz and 15 MHz bandwidth. High and low-gain channels allow for recording both weak bed echoes and strong surface echoes simultaneously and without range-dependent gain control. Coherent data acquisition includes integrations of 16 returned radar signals about every 15 cm along-track. Pulse compression and unfocussed SAR processing using additional along-track integration were significant components of data analysis.

Results: Basal reflection coefficients are computed from these data and then used for inferring the subglacial materials, most notably regions where significant quantities of liquid water are present immediately beneath the ice. However, echo strength statistics based on reflection and scattering theory show that diffuse scattering can still dominate these echoes [8]. Scattering analysis includes imaging of the basal interface at short along-track integration distances to get a low resolution wide look at the basal interface. This is coupled with echo strength statistics (i.e., Rayleigh and Rice criteria) as well as echo amplitude and phase rates of change with distance (i.e., fading). Using the new radar data, we quantify off-nadir scattering from the subglacial interface to infer both the small-scale roughness and the distribution of slopes and facets associated with bottom crevasses and bedrock. We also identify and contrast regions of potential ablation and accretion at the ice-ocean interface.

A similar approach is applied to echoes from the ice-air interface. Reflection and scattering results show regions of heavy surface crevassing, as well as a variation in the surface reflection coefficient consistent with regional changes in firn density. We show that the level of crevassing is also well-quantified by off-nadir surface scattering and/or subsurface volume scattering.

References: [1] Chyba, C. F. et al. (1998) *Icarus*, (134) 292-302. [2] Blankenship, D. D. et al. (1999) *UTIG Tech. Rept. No. 184*. [3] Blankenship, D. D. et al. (2001) *LPSC (32) abstract 1854*. [4] Moore, J. C. (2000) *Icarus* (147) 292-300. [5] Blankenship, D. D. (1989) *EOS*, (70) 1081. [6] Bentley, C. R. et al. (1998) *J. Glaciol.*, (44) 149-156. [7] Moussessian, A., et al. (2000) *Proc. IEEE Intl. Geosci. Rem. Sens. Symp.*, July 24-28, 2002, (2) 484-486. [8] Peters, M. E. et al. *J. Glaciol.* (submitted).

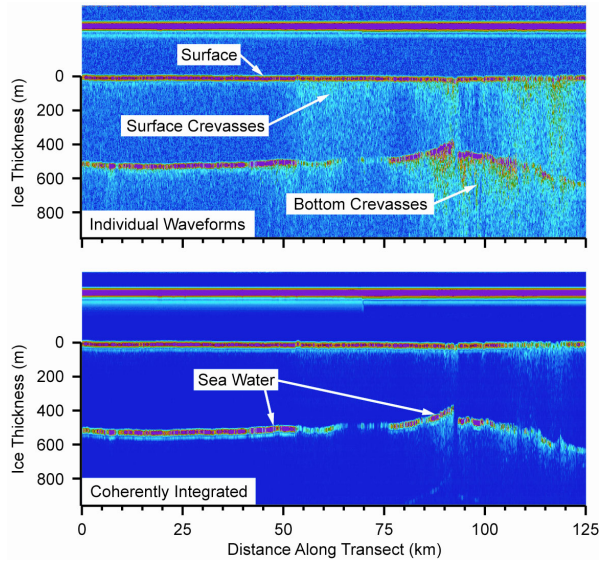


Figure 1. Coherent radar sounding profile at the grounding zone of ice stream C [5,6]. Individual waveforms (top panel) are coherently integrated along-track (bottom panel) implementing unfocussed SAR. Note the crevasse clutter cancellation. The labeled surface crevasses are the relict ice stream C shear margin. The bottom crevasses and overlying surface crevasses are due to tidal flexure at the grounding line.

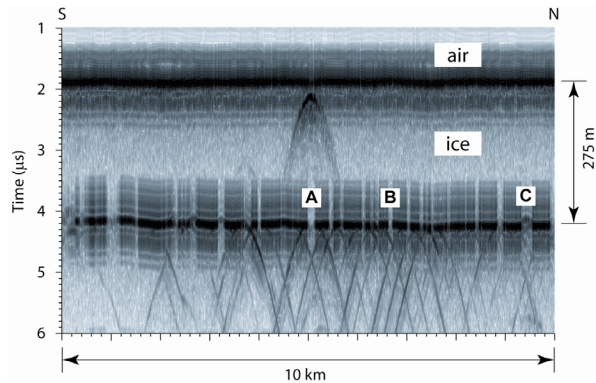


Figure 2. Radar sounding profile across a portion of iceberg B-15. Note the large crevasse (A) extending through the entire ice thickness. Smaller bottom crevasses are also visible and are characterized by echoes up to 20 dB weaker than those for the adjacent ice-ocean interface.

IMPACT GARDENING, SPUTTERING, MIXING, AND SURFACE-SUBSURFACE EXCHANGE ON EUROPA. Cynthia B. Phillips and Christopher F. Chyba, Center for the Study of Life in the Universe, SETI Institute, 2035 Landings Drive, Mountain View CA 94043. phillips@seti.org

Introduction: Charged-particle interactions with materials at Europa's surface can produce biologically useful oxidants such as molecular oxygen and hydrogen peroxide, which could help sustain a biosphere on Europa. Irradiation of carbon-containing materials at the surface of Europa should also produce simple organics [1-5]. These oxidants and organics, if transported downward through the ice shell to a liquid water layer, could provide a significant amount of energy to sustain a biosphere. However, irradiation also destroys such materials if they remain exposed on Europa's surface [6]. Sputtering erosion and surface mixing through impact gardening act to change the preservation depth.

If sputtering dominates over gardening, then material is created and destroyed at Europa's surface much faster than it can be buried and preserved by gardening. However, if gardening dominates, this means that irradiation products can be buried beneath the surface by gardening, where they are protected from further radiation processing. We are investigating models of gardening on Europa's surface to determine which regime is most appropriate. The results of this work will also provide the expected regolith depth on Europa, of relevance for future Europa landing spacecraft.

Once material is preserved from the surface irradiation that would destroy it, it must still work its way down through perhaps a kilometer or more of Europa's icy crust before it could become biologically relevant to a putative ocean biosphere. We begin the investigation of the myriad transport mechanisms that would help bring material from the surface to the potential ocean. These mechanisms will also bring up material from the subsurface to the surface, with relevance for the detection of subsurface composition and potential biosignatures.

Previous Gardening Estimates: Previous estimates of the gardening rate on Europa have depended on various assumptions and scalings, often over orders of magnitude. An initial attempt at a gardening estimate [6] based on a lunar analogy resulted in a gardening depth of about 1-10 centimeters over an expected surface age for Europa of about 10 Myr [7,8].

A later estimate of Europa's gardening rate [4] relied heavily on a regolith depth estimate from studies of Voyager images of Ganymede [9]. It also used a mass flux for small particles from studies of planetary rings [10]. This work resulted in a gardening depth of ~1.3 m over a surface age of ~10 Myr [4].

We have previously attempted to update the gardening rate for Europa by using Galileo data. Our initial attempt [11] used the impactor populations in the outer solar system summarized by Zahnle *et al.* [7,8] combined with lunar regolith growth studies of Shoemaker *et al.* [12,13] and Gault [14] as summarized in Melosh [15]. Based on this approach, we estimated a gardening depth on Europa of about 0.67 meters over a surface age of ~10 Myr [11]

To get this initial estimate, we used a value for the slope of the cumulative crater distribution from [9], which came from lunar studies for craters below 1 km in diameter, but is also consistent with fragmentation cascade studies done for small objects [7].

To update this estimate using Galileo data, we attempted to scale down from the large crater distribution of Zahnle *et al.* [7,8] to get a more relevant value for the slope of the crater distribution (a key parameter in our gardening model [11]).

The problem with this approach was that it required us to assume that the slope of the observed large crater distribution on Europa was continued all the way down to the small sub-meter scale craters that are responsible for gardening. Large crater events on Europa are so infrequent compared to Europa's young surface age that they are fairly irrelevant to the gardening depth (by which we mean the mixing depth averaged over the entire surface). Instead, it is the small, more frequent and widespread cratering events which produce the broken surface layer commonly called regolith on small, airless worlds.

New Gardening Approach: Our current approach follows the same gardening depth formalization as our previous work [11], but instead of scaling down from the large crater distribution, we are using the counts of small craters by Bierhaus *et al.* [16]. These crater counts allow us to determine a small crater distribution from observations rather than by scaling from large craters.

Although we still have to scale down from the craters observed by [16] in the Galileo data (which range in diameter from tens of meters up to a kilometer or so), at least the scaling is over fewer orders of magnitude than was required previously. Also, there appears to be a significant change in slope between small and large craters on Europa, which could be due primarily to the significance of secondary craters on Europa [16]. Since there are so few large primary craters on Europa, Bierhaus *et al.* [16] found that the majority of

small craters on Europa's surface are actually secondary craters from these large impacts. Whether the small craters are primaries or secondaries, however, should not have a large effect on the mechanics of gardening and regolith formation.

Thus, we believe that our new approach, currently in progress, of applying the observed small crater distribution to the models of gardening and regolith formation developed in our previous work [11], will result in a definitive Galileo-era gardening depth estimate for Europa. Since it seems that the sputtering models are fairly mature at this point [4], once we have a final gardening estimate we can compare it to the sputtering estimates to see what the prospects are for the preservation of radiation products at Europa's surface.

Surface – Subsurface Exchange: Once material has been created through radiation processing at Europa's surface and buried below the radiation processing depth by gardening, the material must then make its way down to the ocean layer before it can become biologically relevant. By considering the number of formation models proposed for various geologic features on Europa's surface, we plan to estimate the amount of material that could be transported from the surface to the subsurface ocean layer, as well as the amount of material that could be brought up from a subsurface ocean to the surface or near-surface. We will present a preliminary overview of this work as well.

References:

- [1] Chyba C.F. and Phillips C. B. (2001) *Proc. Natl. Acad. Sci.* **98**, 801-804.
- [2] Chyba C.F. (2000a) *Nature* **403**, 381-382.
- [3] Chyba C.F. (2000b) *Nature* **406**, 368.
- [4] Cooper J.F. et al. (2001) *Icarus* **149**, 133-159.
- [5] Chyba C.F. and Phillips C. B. (2001) *LPSC XXXII*, abs. 2140.
- [6] Varnes E.S. and Jakosky B.M. (1999) *LPSC XXX*, 1082 (CD-ROM).
- [7] Zahnle K. et al. (1998) *Icarus* **136**, 202-222.
- [8] Zahnle K. et al. (1999) *LPSC XXX*, 1776 (CDROM).
- [9] Shoemaker E. M. et al. (1982) The Geology of Ganymede, in *Satellites of Jupiter*, ed. D. Morrison, UA Press, Tucson AZ.
- [10] Cuzzi J.N. and Estrada P.R. (1998) *Icarus* **132**, 1-35.
- [11] Phillips, C.B., and C.F. Chyba (2001) *LPSC XXXII*, abs. 2111.
- [12] Shoemaker E. M. et al. (1969) *JGR* **74**, 6081-6119.
- [13] Shoemaker E.M. et al. (1970) *Proc. Apollo 11 Lunar Science Conference*, v. 3, 2399-2412.
- [14] Gault D.E. (1970) *Radio Science* **5**, 273-291.
- [15] Melosh H. J. (1989) *Impact Cratering: A Geologic Process*. Oxford University Press.
- [16] Bierhaus E.B. et al. (2001) *Icarus* **153**, 264-276.

CLATHRATE HYDRATES IN JUPITER'S SATELLITE EUROPA AND THEIR GEOLOGICAL EFFECTS. O. Prieto-Ballesteros¹, J. S. Kargel², M. Fernández-Sampedro¹ and D. L. Hogenboom³. ¹Centro de Astrobiología. INTA-CSIC. Torrejon de Ardoz, 28850 Madrid. Spain (prietobo@inta.es). ² Astrogeology Team. USGS. Flagstaff, Arizona. USA (jkargel@usgs.es). Lafayette College, Easton Pennsylvania, USA (hogenbod@mail.lafayette.edu)

Introduction: The crust of Europa is dominated by water ice, but some contaminants have been detected on the surface. Several hydrates have been mentioned as part of the composition of the mineralogy of the surface of Europa such as sulfuric acid hydrates [1, 2] and salt hydrates [3, 4, 5, 6]. Clathrate hydrates are also minerals to be considered to be formed in the crust and the possible ocean of Europa.

Physical chemical properties of the hydrates are sometimes substantially different from water ice, so they could locally regulate the final state of the crust and the ocean. Parameters such as thermal conductivity, density and low melting points of these materials are useful to incorporate in the physical geological models of Europa.

Clathrates from brines.

Electrolytes in solution are usually taken as clathrate formation inhibitors. Ions in solution affect the formation of the clathrates in two ways: a) the strong attraction of the water to the electrolytes, and b) the salting-out effect, or the decreasing solubility of the gas molecules into the salty water due to the clustering of the water with the ions. The effects of some chlorides such as NaCl or CaCl₂ in the clathrate formation are already quantitatively known. These systems have been extensively studied experimentally and theoretically because they are frequent in the Earth seawater and in many fluid inclusions of terrestrial rocks.

The composition of water reservoirs in Europa have been proposed to be salty from magnetic data analysis and geochemistry modelling [7, 8, 9]. Sulfate-enriched brines for Europa's water reservoirs have been supported by some studies. Since planetary objects generally also contain and release gases from their solid interiors, various gases are also likely constituents of Europa's ocean and floating icy shell. Unlike most planetary objects, which release their gases onto their surfaces, where they form atmospheres or surface condensates, or else escape into space, Europa's ocean is likely to contain vented gases up to the limit of high-pressure saturation. Free fluid phases can form and then may be vented as gases through the icy shell. However, ocean saturation of small apolar gas molecules generally should result in formation of clathrate hydrate phases.

Candidate guest molecules to form clathrates in Europa are CO₂ and SO₂, both observed on the surfaces of some Galilean satellites [10, 11] and are geochemically plausible [5, 12]. Other likely clathrate-forming guest molecules in Europa's ocean and icy shell may include N₂ and perhaps O₂ (the latter from radiolytic processes), and possibly CO and CH₄. CO₂ is especially likely and probably abundant, because it is observed and abundant from Venus to the most distant realms of the Solar System, including comets. SO₂ may be abundant on Europa if Europa's rocky interior and the geochemical processing there is anything like that of Io.

We use a modification of the Hammerschmidt equation (eq. 1) [13, 14] to calculate an approximation of the effect of the magnesium sulfate to the formation of CO₂ clathrates at constant pressure as an example of how salts may affect clathrate stability in Europa:

$$\left(\frac{1}{T_d^0} - \frac{1}{T_d} \right) = \frac{n \cdot \Delta H_{FUS(I)}}{\Delta H_{DIS}} \left(\frac{1}{T_f^0} - \frac{1}{T_f} \right) \quad (\text{eq. 1})$$

where: T_d^0 and T_d are the temperatures at which CO₂ dissociates in pure water and in the solution, ΔH_{DIS} is the enthalpy of dissociation of CO₂ clathrate, n is the number of water molecules in hydrate formula, $\Delta H_{FUS(I)}$ is the enthalpy of fusion for pure ice and T_f^0 and T_f are the melting temperatures of ice and the electrolyte solution.

The result (Fig. 1) indicates that dissolved magnesium sulfate decreases the crystallization point of the clathrate in a similar manner to the way the salt itself reduces the melting point of water ice.

Geological implications: The presence of large amounts of hydrates (clathrates, sulfuric acid or salt hydrates) produce some effects on the geology of Europa. Clathrate and salt hydrates have low thermal conductivities, as some experimental analyses indicate [15, 16]. If they are present in the icy crust they would

produce zones of high thermal gradient and perhaps enhanced geological activity of several types.

As has been theoretically predicted, CO₂ clathrates may crystallize from salty water reservoirs at lower temperatures than from pure water. The inhibition of formation only amounts to about 2 K at the eutectic proportions of MgSO₄ (17%). On one hand, this means that insofar as clathrates are concerned, the salts do not have a large effect. On the other hand, the introduction of clathrate-forming gases into a salt-saturated or undersaturated ocean may have a large effect on the salts. Formation of clathrates removes water from the solution, so there will be a higher concentration in ions as soon as the clathrates are formed. This property has been used to desalinate terrestrial seawater. If this process occurs in an aqueous magmatic chamber in the crust of Europa, clathration could result in a cryomagmatic differentiation. The formation of clathrates would separate the crystals from the more concentrated brine magma by density. If the destruction of the clathrate layer occurred by any movement or fracturation, clean water ice could ascend through the brine to higher levels.

Destruction of clathrate layers near the surface could produce catastrophic processes because of the fast liberation of gases, and the large negative volume change of the solid phases upon dissociation and loss of the free gas phase. Fracturing and gravitational collapse of terrain could ensue. It could be an autocatalytic, even catastrophic process if fracturing and depressurization causes more clathrate to dissociate and especially if gas-saturated brine from the ocean jets through fractures and erosionally widens them. Chaotic terrain on Europa could conceivably be related to this process, as it may also on Mars, Earth, and Triton [17]. That also could be responsible for explosive cryovolcanic events, as some authors have already pointed out [17, 18, 19].

The transition from a condensed phase (such as clathrate) to a multiphase system containing a free vapor phase is always endothermic if chemical reactivity is not involved (as with clathrate dissociation forming a free vapor phase). Therefore, cooling and crystallization of ice (possibly also salts if the system is already salt-saturated) will occur during dissociation of ice-equilibrated clathrates (as Europa's are expected to be). However, the system includes a negative volume change of the condensed phase assemblage if the free vapor phase is vented; therefore, a continuing fracturing process and collapse of the system can occur in a runaway process of chaotic terrain formation. Energy for the process can be supplied by effervescing oceanic brine gushing through and widening the fractures.

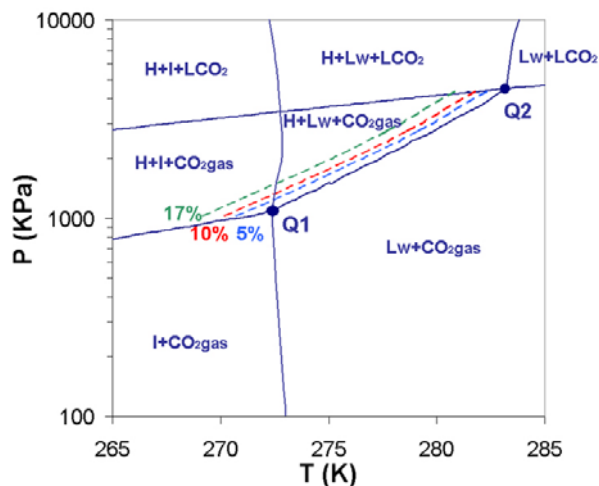


Figure 1. Phase transition diagram of CO₂ clathrate. Colors show the displacement of the stability line of clathrates, if the indicated proportions of MgSO₄ are added to the aqueous solution. H= clathrate hydrate, I = water ice Lw=liquid water, LCO₂= liquid CO₂, Q1 and Q2 are the quadruple points.

References:

- [1] Carlson, R.W. et al (1999). *Science* 286, 97-99. [2] Carlson, et al. (2002). *Icarus* 157, 456-463. [3] Fanale, F.P. et al. (2001). *J. Geophys. Res.* 106, 14,595-14,600. [4] Kargel, J. S. (1991). *Icarus* 94, 368-390. [5] Kargel, J. S., et al. (2000). *Icarus* 148, 226-265. [6] McCord, T. B., et al. (1999). *J. Geophys. Res.* 104, 11,827-11,851. [7] Kargel, J. S. and G. J. Consolmagno (1996). *LPSC XXVII*, 643-644. [8] Khurana, K. K., et al. (1998). *Nature* 395, 777-780. [9] Kivelson, K. G., et al. (1999). *J. Geophys. Res.* 104, 4609-4626. [10] Hibbitts, C. A. et al. (2000). *J. Geophys. Res.* 105, 22541-22557. [11] Lane, A. L., et al. (1981) *Nature* 292, 38-39. [12] Crawford, G. D. and Stevenson, D. J. (1988). *Icarus* 73, 66-79. [13] Sloan, E. D. (1998) In: *Clathrate hydrates of natural gases*. Marcel Dekker Inc., NY. [14] Dickens, G. R. and Quinby-Hunt, M. S. (1997). *J. Geophys. Res.* 102, 773-784. [15] Prieto-Ballesteros, O. and Kargel, J. S. (2002). *LPSC XXXIII*, n° 1726. [16] Ross, R. G. and J. S. Kargel (1998). In *Solar System Ices*, (B. Schmitt, C. De Berg y M. Festou Eds.), pp. 33-62. Kluwer Academic Publishers, Netherlands. [17] J.S. Kargel, et al. (2003) *Geophys. Res. Abstracts*, 5, 14252, 2003, European Geophysical Society. [18] Fagents, S. A. et al. (2000). *Icarus* 144, 54-88. [19] Stevenson, D. J., (1982). *Nature* 298, 142-144.

GEOLOGICAL FEATURES AND RESURFACING HISTORY OF EUROPA. L. M. Prockter¹ and P. H. Figueredo², ¹Applied Physics Laboratory, Laurel, MD 20723, Louise.Prockter@jhuapl.edu, ²Department of Geological Sciences, Arizona State University, Tempe, AZ 85287, figueredo@asu.edu.

Introduction

Many different models have been proposed for the formation of Europa's primary surface features: ridges, bands, chaos and lenticulae. We briefly review the models, evaluating their strengths and weaknesses, and their implications for the thickness of Europa's ice shell. We discuss Europa's stratigraphy, and how the surface may have evolved through time.

Morphological features

Ridges: Double ridges are without doubt the most ubiquitous feature on Europa's surface. They are highly unusual in the solar system, and have only been identified on Triton to date [1]. The European ridges constitute an intricate mesh, they have formed throughout Europa's visible history and may still be forming today [e.g., 2]. Ridges appear to form a genetic sequence of different morphological types, ranging from simple troughs, through double ridges, then triple ridges, and finally any number of closely spaced ridges, termed "ridge complexes" [2, 3]. The dominant type by far is the double ridge, which has two crests of largely uniform width and height, separated by a V-shaped trough. Ridges range in size, from ~500 hundred m to ~2 km wide, up to ~200 m high, and up to several thousand km in length, meaning that some are hemispherical in scale. Cycloidal ridges appear to form on relatively rapid timescales resulting from Europa's diurnal cycle [4], but the details of how the majority of Europa's ridges are created are still open to debate.

Several models have been proposed for the formation of the ridges, each of which has its strengths and weaknesses. These include: (1) *Tidal squeezing*, in which fractures penetrate through an ice shell, and open and close as a result of diurnal stresses [5]. The amount of opening and closing is small – about 1 m – and each cycle allows water and icy slush to be pumped toward the surface, forming the characteristic ridge crests and central trough. This process is similar to that which forms terrestrial pressure ridges in lead ice, and the morphology is remarkably similar. (2) *Compression*, in which ridges are proposed to have a compressional origin [6]. This model could help account for the mystery of Europa's surface, which has abundant evidence of extension, but little identified compression. While falling out of favor for a few years, this model has recently been revived by [7]. (3) *Linear volcanism*, in which ridges are proposed to be the result of gas-driven fissure eruptions, resulting in ridge crests comprised of cryoclastic debris [8]. Volatiles SO₂ and CO₂ could drive the eruptions. (4) *Linear*

diapirism, a model in which ridges are proposed as the surface expression of linear warm ice diapirs, which rise to the surface, causing cracking and uplift of the surrounding terrain, forming ridge flanks [9]. (5) *Dike intrusion*, in which ridges form by intrusion of melt into vertical cracks, resulting in plastic deformation to form ridge morphology [10]. (6) *Shear heating*, in which heating along cracks from diurnal strike-slip motion causes upwelling of warm ice to form ridges, with possible associated partial melting [11]. To date, none of these models can describe all the features characteristic of ridges, such as uniformity in space and time, forks, and sharp turns.

Bands: Bands are features up to tens of km wide and hundreds of km long, which apparently brighten with age. They have formed through complete separation of the preexisting surface, by extension, shear and/or compression [12, 13]. Two primary models have been proposed for the formation of bands. The first suggests that they are a continuation of the tidal-squeezing ridge forming process [5], and that they result from continuous ratcheting apart of a crack due to diurnal stresses and the possible influence of secular variations [14]. The rising water is proposed to freeze, preventing the crack from closing, and is then pulled further apart during the next tidal cycle, adding more frozen material and widening the band. This model implies that Europa's ice shell is relatively thin. The second model proposes that bands have an origin similar to that of mid-ocean ridges [15], and that they form from solid-state material, possibly ductile warm ice [16]. As with the previous model, new material is added along the band's central axis, but it is solid state, and the resulting band morphology may depend on the rate of band opening. This model does not require a thin shell.

Lenticulae: Lenticulae are the many subcircular areas of disrupted terrain present across Europa's surface. They range in size but are generally agreed to cluster around ~10 km in diameter [e.g., 2, 17]. Lenticulae can be either pits, domes, low albedo plains areas, or some combination of these. Many of them (known as microchaos) have interiors which are broken into small plates of preexisting surface material in a lower albedo matrix [2]. Two primary models have been proposed for their origin. The first, based on their apparently uniform size distribution, suggests that they are the result of diapirism [18, 19], possibly due to thickening of the ice shell to a point at which convection can be initiated. The second, based on the resem-

blence of plates within the lenticulae to terrestrial icebergs, suggests that they result from melting of the surface by liquid water [20, 21] requiring a much thinner shell. Lenticulae may be related to the formation of chaos.

Chaos: Chaos regions are much larger than lenticulae, but are also areas of Europa's surface that appear to have been significantly disrupted by some endogenic (cryo)magmatic process. Although there are morphological variations, chaos terrain is comprised of polygonal plates of preexisting surface material, in a dark, finer grained hummocky matrix [2]. In at least one area, there is evidence that the plates have shifted from their original position [22], and chaos may stand either higher or lower than its surroundings [2, 23]. As with the lenticulae, the two models proposed for chaos formation are that they formed from regions of liquid water melt-through [20, 21], or from single or merged diapirs of warm ice [18]. Each model has significant implications for the thickness of the shell.

Resurfacing history

Image coverage and resolution from the Galileo spacecraft has been sufficient to allow several local and regional areas on Europa to be mapped, and a stratigraphy to be derived [2, 24]. Recent pole-to-pole mapping [25] considerably extends earlier work over a much broader area of coverage, and confirms previous suggestions that there has been an apparent change in the style of resurfacing on Europa over time. The visible history of Europa only goes back as far as the "background ridged plains" which comprise most of Europa. This unit is so heavily tectonized that it is very hard to determine the existence of any preexisting features within it; Europa has either been completely resurfaced prior to background plains formation, or features that existed prior to its formation are so completely tectonized as to be unrecognizable. Either way, the average surface age of Europa is estimated to be ~60 Ma [26].

Postdating the formation of the background plains, the next oldest group of features are the gray bands. Bands have a variety of orientations and commonly cross-cut each other, but none appear to have formed in Europa's recent history. Whether formed from liquid water or warm ice, they suggest a change in resurfacing style to magmatic processes. Chaos and lenticulae commonly postdate bands, although it is impossible to tell whether they themselves formed concurrently. Since chaos-related features are some of the youngest units in Europa's stratigraphic column, it is possible that they are still forming today. This inference has significant implications for Europa's astrobiological potential, since such features may be places where its ocean communicates with the surface. Dou-

ble ridges and craters are found throughout Europa's visible surface history, although tectonic lineaments have been found to narrow over time, perhaps indicating a change in the thermal state of Europa's ice shell [25].

The change in the formation from bands (lateral tectonics with associated cryomagmatism) to chaos (vertical transport of cryomagmatic materials) has been suggested as evidence that Europa's shell may be undergoing progressive thickening with time, possibly as a result of the "freezing out" of an ocean [16, 24, 25, 27]. Such thickening may explain the change from the inferred earlier mobility of the ice shell, in which lithospheric separation, and hence band formation, was common, to a convective state in which lenticulae and chaos are the norm.

The apparent change in Europa's resurfacing style is not sufficient to place this transition into a longer-term context [25, 27]. Because Europa's surface is so young, on average, we cannot tell from currently available data whether the apparent thickening of the ice shell corresponds to the complete cessation of geological activity, whether both processes coexist in different regions, or whether there are cycles of alternating tectonic and cryovolcanic activity, on geological timescales.

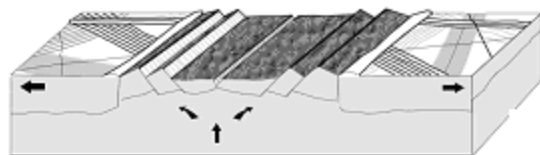
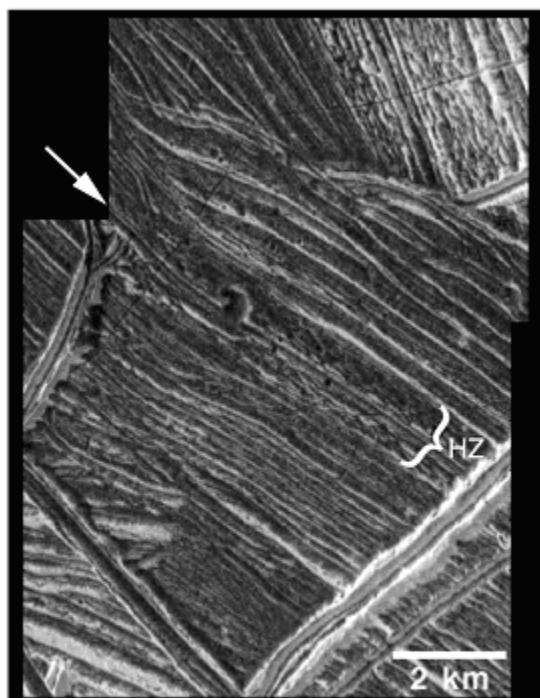
References:

- [1] Croft et al. (1995) Neptune and Triton, ed. D.P. Cruikshank, U. of Arizona Press, Tucson, p. 879-948. [2] Greeley, R., et al. (2000) *J. Geophys. Res.*, 105, 22,559-22,578. [3] Pappalardo, R.T., et al. (1998) *LPSC XXX*, 1859. [4] Hoppa, G., et al. (1998), *Science*, 285, 1899-1902. [5] Greenberg et al., *Icarus*, 135, 64-78, 1998. [6] Sullivan, R., et al., (1999) *LPSC XXX*, CD-ROM 1925 [7] Patterson, G. & R. Pappalardo, (2002), *LPSC, XXXIII* CD-ROM 1681. [8] Kadel S. et al., (1998), *LPSC XXX* CD-ROM 1078; Fagents et al., (2000), *Icarus* 144, 54-88. [9] Head J., et al., (1999), *J. Geophys. Res.*, 104, 24,223-24,236. [10] Turtle E. et al. (1998), *EOS* 79, F541. [11] Gaidos, E., & F. Nimmo (2000), *Nature* 405, 637. [12] Schenk P. & W. McKinnon, (1989), *Icarus*, 79, 75-100. [13] Sarid, A., et al., (2002), *Icarus*, 158, 24-41. [14] Tufts B. et al., (2000), *Icarus*, 141, 53-64. [15] Sullivan, R. et al., (1998), *Nature*, 391, 371-372. [16] Prockter, L. et al., (2002), *J. Geophys. Res.*, 107, 10.1029/2000JE001458. [17] Spaun N., et al., (1999), *LPSC XXX*, CD-ROM 1847. [18] Pappardo R. et al., (1998) *Nature*, 391, 365-366. [19] Rathbun, J. et al., (1998), *Geophys. Res. Lett.*, 25, 4157-4158. [20] Carr, M. et al., (1998), *Nature*, 391, 363-364. [21] Greenberg R., et al., (1999), *Icarus* 141, 263-286. [22] Spaun N. et al., (1998), *Geophys. Res. Lett.*, 25, 4277-4290. [23] Collins G. et al., (2000), *J. Geophys. Res.*, 105, 1709-1716; Figueredo P., et al., (2002) *J. Geophys. Res.*, 107, 2-12. [24] Prockter L. et al., (1999) *J. Geophys. Res.*, 104, 16531-16540; Figueredo P. & R. Greeley (2000), *J. Geophys. Res.*, 105, 22629-22646; Kadel S. et al., (2000), *J. Geophys. Res.*, 105, 22656-22669. [25] Figueredo P. and R. Greeley, (2003) *Icarus* in press. [26] Schenk P. et al., in "Jupiter and her Satellites" ed. F. Bagenal (2003), in press. [27] Pappalardo et al., (1999) *LPSC XXX* CD-ROM 1859.

EUROPAN BANDS FORMED BY STRETCHING THE ICY CRUST: A NUMERICAL PERSPECTIVE.

Ran Qin¹, W. Roger Buck¹, Robert T. Pappalardo², ¹Lamont-Doherty Earth Observatory of Columbia University, Palisades, NY 10964, email: rqin@ldeo.columbia.edu; ²Department of Astrophysical and Planetary Science, University of Colorado at Boulder, CO

High-resolution Galileo images of Europa show linear, curved and wedge-shaped bands crossing the ice surface. These bands are most clearly seen within the region southwest of Europa's anti-Jovian point and make up ~60% of the terrain[1]. It has generally been inferred that bands have formed in response to extension, although Schulson [2] suggests that at least one wedge-shaped band may have formed under compressive stress, analogous to small-scale "wing cracks".



Reconstruction of bands implies that Europa's surface layer has behaved in a brittle or plastic manner, separating and translating atop a low-viscosity subsurface material, with the gap being infilled with relatively dark, mobile material. Two principal models have been proposed for band origin. If Europa's ice shell is very thin (<6 km) and cracks can penetrate through the entire ice shell, then a model of extrusion of water and slush during band opening may be applicable[3][4]. On the other hand, if Europa's ice shell is thicker and ductile subsurface ice plays a significant role in shaping the satellite's geology [5], then bands may have formed from relatively warm ice and would be more analogous to terrestrial mid-ocean ridge rift zones[1][6]

One endmember of Europa's bands commonly exhibit prominent axial troughs, symmetrical spreading from a central axis, large hummocks, tilted fault blocks and bounding ridges (Fig. 1), several kilometers wide and up to 100 meter higher than the surrounding plain. Broadly analogous morphological feature types are also found along terrestrial mid-ocean ridges in the form of axial graben, features of the neovolcanic zone, and abyssal hill normal faults [7]. On the basis of morphology and inferred topography within the bands (such as axial troughs and linear ridges), Prockter et al. [1] proposed that a terrestrial seafloor spreading analog may be appropriate for European bands. Furthermore, these authors speculated that if the bands on Europa are analogous to terrestrial mid-ocean ridges and a similar mode of formation applies to both, then analogous processes may be the cause of variations in morphology and topography among the European bands.

Terrestrial slow spreading ridges generally exhibit prominent axial troughs, large faults and numerous volcanic edifices as new material is slowly formed then rafted away from the central spreading axis. If on Europa, these characteristic bands (Fig. 1) have opened relatively slowly forming cooler, thicker lithosphere close to the axis, allowing significant topography to be supported, this would be analogous to those slow-spreading mid-ocean ridges such as the Mid-Atlantic Ridge.

We are currently adapting a sophisticated numerical model that exists for modeling rifting phenomena on Earth, as developed and first applied to slow-spreading mid-ocean ridge abyssal hill topography by Buck and Poliakov [8], to quantitatively test the hypothesis of European hummocky band formation by stretching its icy crust. The numerical model uses an explicit finite-element method similar to the FLAC (Fast Lagrangian Analysis of Continua) technique of

Cundall [9]. The Lagrangian method allows us to trace the material flow and a remeshing technique is developed to adjust the numerical grid when it's heavily deformed. Advection and diffusion of heat are also included to allow a time varying lithospheric structure. The surface temperature of Europa is around 100 K and increases toward its interior following a proper temperature gradient, probably 5 ~ 40 K/km. The ice of Europa is commonly believed to have elastic-viscoplastic rheology [10][11] which is temperature and strain-rate dependent. In the shallow, cold part of this layer the viscosity is so high that it effectively behaves as a brittle material, approximated with Coulomb elastoplastic rheology, which allows for localization of shear deformation that mimics faults. Warmer regions deform by thermally activated creep. This numerical model will allow us to explore relationships among opening rate, cooling rate, fault initiation, and morphology of rift zones that might be formed by stretching of Europa's icy crust.

Preliminary model runs have been performed with coarse grids to ensure that our algorithms--developed to model faulting in terrestrial rock--will succeed in reproducing tectonic structures in ice. These preliminary runs have successfully produced faults within a thin ice lithosphere with, a transition from brittle to ductile behavior occurring near 0.5 to 3 km (the range constrained observationally [5]), and faults penetrating to near this depth. These results, however, are not yet fully validated. This main goal of our modeling is to produce the surface morphology that will be compared to the morphologies of bands on Europa. Our results will address the first-order question of whether the mid-ocean ridge analog model is an appropriate one to apply to Europa, and if so, will constrain the formation conditions appropriate to formation of bands, notably thermal structure and strain rate.

References: [1]Prockter, L. M. et al. (2002) Morphology of European bands at high resolution: A mid-ocean ridge-type rift mechanism, *J. Geophys. Res.*, 107(E5), 10.1029/2000JE001458. [2]Schulson, E.M. (2002) On the origin of a wedge crack within the icy crust of Europa, *J. Geophys. Res.*, 107(E11), 10.1029/2001JE001586. [3]Greenberg, R. et al. (1998) Tectonic processes on Europa: Tidal stresses, mechanical response, and visible features, *Icarus*, 135, 64-78. [4]Tufts, B. R. et al. (2000) Lithospheric dilation on Europa, *Icarus*, 146, 75-97. [5]Pappalardo, R. T. et al. (1999) Does Europa have a subsurface ocean? Evaluation of the geological evidence, *J. Geophys. Res.* 104, 24015-24055. [6]Sullivan, R. et al. (1998) Episodic plate separation and fracture infill on the surface of Europa, *Nature*, 391, 371-372. [7]MacDonald, K.C. (1982) Mid-ocean ridges: Fine scale tectonic, volcanic, and hydrothermal processes within the plate boundary zone, *Ann. Rev. Earth Planet. Sci.*, 10, 155-190. [8]Buck, W. R. and A. N. B. Poliakov (1998) Abyssal hills formed by stretching of oceanic lithosphere, *Nature*, 392, 272-275. [9]Cundall, P.A. (1989) Numerical experiments on localization in frictional materials, *Ingenieur-Archiv*, 58, 148-159. [10]Durham, WB and LA Stern (2001) Rheological properties of water ice – application to satellites of the outer planets, *Annu. Rev. Earth. Planet. Sci.*, 29, 295-330. [11]Schulson E.M. (2001) Brittle failure of ice, *Engineering Fracture Mechanics*, 68, 1839-1887.